HHS Public Access

Author manuscript

J Biomed Mater Res A. Author manuscript; available in PMC 2020 March 23.

Published in final edited form as:

J Biomed Mater Res A. 2019 September ; 107(9): 1954–1964. doi:10.1002/jbm.a.36706.

The improvement of cell infiltration in an electrospun scaffold with multiple synthetic biodegradable polymers using sacrificial PEO microparticles

Jacob Hodge, **Clay Quint**

Department of Surgery, University of Kansas Medical Center, Kansas City, Kansas

Abstract

Electrospinning is a fabrication technique to generate three dimensional scaffolds with a fiber structure that imitates extracellular matrix for tissue engineering constructs. The versatile characteristics of the electrospinning process yields designer scaffolds made of biodegradable polymers or natural proteins with controllable fiber diameters, biodegradation, and mechanical properties. A limitation of conventional electrospun scaffolds is the dense fiber packing with low porosity that leads to poor cell infiltration. Electrospraying sacrificial polyethylene oxide (PEO) microparticles in combination with electrospun scaffolds are a method to increase porosity. We report the effectiveness of electrospraying PEO microparticles to increase porosity of the most commonly used biodegradable polymers: polyglycolic acid (PGA), poly (lactic-co-glycolic) acid (PLGA), and polycaprolactone (PCL). The biodegradable polymer electrospun scaffolds with the sacrificial PEO microparticles were found to have improved cell proliferation and infiltration with human fibroblasts compared to conventional electrospun scaffolds. The mechanical properties of the more robust PGA and PLGA had minor changes, but the more elastic PCL was observed to be weaker and less stiff after the removal of the PEO microparticles. Therefore, this study found PEO microparticles can increase porosity and cell infiltration with stable mechanical properties for a wide variety of biodegradable polymers in electrospun scaffolds.

Keywords

cell infiltration; electrospun; PCL; PEO microparticle; PGA; PLGA

1 | INTRODUCTION

Tissue engineering integrates principles of engineering and biomedical sciences to improve tissue function of diseased organs (Langer & Vacanti, 1993). The components of a tissue engineered device are a biomaterial to function as a scaffold, a cell source, and a method to induce tissue growth (Langer & Vacanti, 1993). The role of the scaffold for the tissue engineered device is to provide a 3D substrate for the cells to generate an extracellular matrix that eventually forms neotissue. The properties of the scaffold are crucial for the cell proliferation, migration, differentiation, and mass transport that will determine cell function

Correspondence: Clay Quint, Department of Surgery, University of Kansas Medical Center, Kansas City, KS 66160. cquint@kumc.edu.

and production of extracellular matrix. There are a variety of methods to fabricate 3D structures, such as melt molding, extrusion, phase separation, self-assembly, bioprinting, and electrospinning (Carletti, Motta, & Migliaresi, 2011). Depending on the type of tissue engineering application, there may be specific requirements that favor one technique over another in terms of architecture, mechanical properties, biodegradation, and biocompatibility. Tissue engineering through the use of novel scaffolds has the potential to offer new medical therapies that are superior to current prosthetic materials by incorporating into the surrounding tissue.

The most optimal scaffold would be to create a structure that resembles the natural extracellular matrix of the tissue to allow for cellular regeneration. Properties that would replicate the native tissue are fibers with similar sizes to extracellular matrix proteins (100–500 nm) and the incorporation of natural proteins into the synthesized scaffold (Barnes, Sell, Boland, Simpson, & Bowlin, 2007). Electrospinning is a flexible method that continues to expand into tissue engineering applications because of the ability to generate a nanofiber structure with a wide range of synthetic and natural proteins to tailor the properties of the scaffold for the requirements of the tissue. Electrospinning forms nanofibers by injecting a polymer solution through a high voltage field that collects on a grounded surface (Agarwal, Wendorff, & Greiner, 2009). A wide variety of synthetic biodegradable polymers have been used for electrospinning, including polycaprolactone (PCL), poly(lactic) acid (PLA), Poly(lactic-coglycolic) acid (PLGA), polyglycolic acid (PGA), and polydioxanone (Li, Cooper Jr., Mauck, & Tuan, 2006; Sell et al., 2006). Natural proteins have been incorporated into electrospun scaffolds to improve the cell migration with collagen, elastin, silk fibroin, and gelatin (Li et al., 2005; Matthews, Wnek, Simpson, & Bowlin, 2002). In addition to the flexibility of biomaterials to alter the mechanical properties of the electrospun scaffold, the fiber properties and organization can be modulated based on the conditions of electrospinning. The fiber morphology can be controlled by altering parameters such as solution properties (i.e., concentration, polymer molecular weight), process conditions (i.e., flow rate, voltage potential, distance of the needles), and environmental conditions (i.e., temperature, humidity; Pham, Sharma, & Mikos, 2006). Therefore, electrospinning has advantages compared to other biomaterial fabrication methods because of the ultrafine fiber structure with a large surface-to volume ratio that promotes cell adhesion and proliferation.

Pore size and packing density are the most important factors for cellular infiltration and mass transport for the formation of extracellular matrix on an electrospun scaffold. However, a limitation of the electrospinning process is the dense packing of the fibers with a small pore size that inhibits cellular infiltration. Several studies have shown the optimal pore diameters should be on the same magnitude as the dimensions of the cell to enhance cellular infiltration (Balguid et al., 2009; Zander, Orlicki, Rawlett, & Beebe Jr., 2013). In electrospinning, fiber diameter is a critical factor that can be fine-tuned to alter the pore size in the scaffold (Balguid et al., 2009; Ju, Choi, Atala, Yoo, & Lee, 2010). Therefore, a common strategy to improve cellular infiltration throughout the electrospun scaffold is to increase fiber diameter (often low micrometer rather than nanometer scale) by adjusting the concentration of the fiber solution (Ju et al., 2010). Although fiber alignment and packing density are also related to fiber diameter, it is more difficult to significantly modify the packing density by fiber diameter or process conditions. Thus, methods to adjust pore size

and packing density to retain the structural requirements and encourage cellular infiltration in the electrospun scaffold remain a challenge.

A number of techniques have been recently developed to control porosity of electrospun scaffolds to overcome the limitations of cellular infiltration. There is a balance of removing a sacrificial component to enhance cell infiltration while maintaining structural stability of the electrospun scaffold. Examples of sacrificial components include polyethylene oxide (PEO), salt crystals, and ice crystals (Wu & Hong, 2016). An important consideration with the use of a sacrificial polymer or crystal is a homogenous distribution to prevent irregular pores with areas of either too high or too low porosity. PEO is the most commonly used sacrificial chemical porogen because it can easily be electrospun, and it rapidly dissolves in an aqueous medium (Baker et al., 2008). Several studies have shown that coelectrospinning PEO with PCL can increase porosity after removal of the PEO fiber (Baker et al., 2008; Phipps, Clem, Grunda, Clines, & Bellis, 2012). Further, the number of cells that migrated into the electrospun scaffold has been demonstrated to increase as the PEO content increases in the electrospun scaffold (Baker et al., 2008). Although the cell infiltration improved with the removal of the sacrificial fiber, the tensile properties were found to decrease in a linear fashion as the PEO content was removed (Baker et al., 2008). An alternative to electrospinning PEO has been to use an electrospraying technique to deposit microparticles that provides an even distribution of microparticles at a controlled rate and size. The technique of electrospraying in combination with electrospinning has been shown to increase porosity and cell infiltration for both PCL and silk fibroin (Wang et al., 2013; Wang et al., 2014). Although salt crystal and ice crystal methods can increase porosity by removing the crystals, a uniform pore size and even distribution are challenging to achieve (Leong, Rasheed, Lim, & Chian, 2009; Nam, Huang, Agarwal, & Lannutti, 2007). The ice crystal approach also requires a more advanced electrospinning set-up whereby temperature and humidity control are important variables during the electrospinning process.

In this study, commonly used synthetic biodegradable polymers (PGA, PLGA, PCL) were electrospun while simultaneously electrospraying PEO microparticles to increase the porosity after removal of the PEO microparticles. The unique aspect of this paper was to directly compare electrospun scaffolds using the most common biodegradable polymers in terms of scaffold properties and cell infiltration response after the removal of the PEO microparticles. We hypothesized that the increase in porosity after removal of the PEO microparticle would increase cellular infiltration for all the synthetic biodegradable polymers and retain structural stability. The fiber properties and biodegradation was not expected to change after removal of the electrosprayed PEO.

2 | MATERIALS AND METHODS

2.1 | Fabrication of scaffold

The biodegradable polymers were dissolved in 1,1,1,3,3,3-fluoro 2-propanol (HFIP; Oakwood Chemical, Estill, SC) to obtain the following concentrations (w/v): 12% Polyglycolic Acid (PGA; Teleflex, Coventry, CT), 20% Poly Lactic-co-Glycolic Acid (PLGA, 75:25, Mn 76,000 – 115,000; Evonik, Darmstadt, Germany), 12% Polycaprolactone (PCL; Mn 80,000; Sigma-Aldrich, St. Louis, MO). The polymer solutions were electrospun

using a custom electrospinning device. The polymer solutions were placed in a 10 mL syringe and delivered by a syringe pump (Infusion Syringe Pump, Richmond, CA) that was connected to 18 gauge stainless steel blunt needle at a rate of 4 mL/hr. A high voltage power supply (ES30P-5 W, Gamma High Voltage Research Inc, Ormand Beach, FL) was used to apply a + 15 kV potential difference between the needle and the grounded rotating mandrel. The grounded mandrel was rotating at 2000 RPM at a distance of 12 cm from the needle tip. To fabricate the electrospun biodegradable polymer and the electrosprayed PEO microparticle, the electrospun polymer and the electrosprayed PEO were simultaneously collected on the rotating mandrel at 180˚geometry with the custom built electrospinning device. Polyethylene oxide (PEO; Mn 8,000; Sigma-Aldrich, St. Louis, MO) was dissolved in chloroform (Sigma Aldrich, St. Louis, MO) with stirring overnight at a concentration of 120% w/v. The PEO solution was placed in a 10 mL syringe and was delivered by a syringe pump through a 15 gauge stainless steel blunt needle at a rate of 4 mL/hr with a voltage difference of +12 kV. The distance from the grounded mandrel to the needle tip was 15 cm. The electrospun scaffolds were removed from the mandrel as a tubular structure. The composite scaffolds with the PEO microparticles were rinsed in a series of graded ethanol solutions (100, 90, 80, 70% v/v) for 1 hr each, and then rinsed in deionized water and dried in a hood for 24 hr.

2.2 | Characterization of the scaffolds

The morphology of the electrospun scaffolds (PCL, PLGA, PGA) and the composite electrospun scaffolds before and after removal of the PEO microparticles were sputter-coated with gold for 1 min. The fibers were examined using a scanning electron microscope (*SEM*, Hitachi S-2700). Fiber diameters were measured using image analysis software (Image J, National Institute of Health). Twelve randomly selected fiber diameters were measured on four independent scaffolds for each biomaterial, thus a total of 48 fibers were measured to obtain the average fiber diameter for each electrospun scaffold. Porosity (ε%) was determined using apparent density of the scaffold and standard density. The porosity, $\varepsilon\% = (1-\rho/\rho_o)$, where ρ is the apparent density and ρ_o is the standard density ($n = 6$). The standard density of each biodegradable polymer (PCL, PLGA, PGA) was known from the manufacturer. The apparent density of the electrospun scaffold was determined by dividing the weight of the electrospun scaffold by the volume of the scaffold. The volume was obtained by measuring a scaffold ringlet with digital calipers for the length and width. The thickness was more precisely measured using a microscope. The mechanical properties were determined with uniaxial tensile testing by taking a ringlet and the average three measurements of the thickness, length, and width. The ringlet samples were loaded on an Instron 3,342 device with hooks that attached to the grips with a 100 N load cell. The sample was extended to failure with a crosshead speed of 0.5 mm/s. The ultimate tensile strength, Young's modulus, and elongation at break were obtained from the stress-stain curves ($n = 3$). Chemical analysis of PGA, PLGA, and PCL and the respective polymers before and after PEO removal was performed by attenuated total reflectance-Fourier Transform Infrared Spectroscopy (FTIR; Perkin Elmer Spectrum 400) over a range of 4,000–400 cm^{-1}. Physical analysis of PGA, PLGA, and PCL after removal of the PEO was performed using thermogravimetric analysis (TGA, Perkin Elmer Pyris1) at a rate of 20˚C/min over a range of 0 to 700˚C.

2.3 | Degradation of the scaffold

The degradation of the PGA, PLGA, and PCL were compared to each polymer after the PEO microparticle was removed. Tubular scaffolds were placed in 37˚C in Phosphate Buffer Solution (PBS; Gibco, Grand Island, NY). The tubular scaffolds were assessed by weight and *SEM* at time intervals of 1, 2, and 4 weeks. The dry weight of each scaffold was initially measured, and then re-measured after drying at 1, 2, and 4 weeks to obtain the percent weight change ($n = 3$). Each sample was evaluated with *SEM* as described previously.

2.4 | Cell culture and seeding of the scaffold

The hDFb (Lonza, Walkersville, MD) cells were cultured in DMEM medium (Gibco, Grand Island, NY) supplemented with 10% v/v fetal bovine serum (Gibco, Grand Island, NY) with 1% v/v of penicillin/streptomycin (Gibco, Grand Island, NY) antibiotics at 37˚C and 5% CO_2. Tubular scaffolds 2 cm in length were sterilized with 100% ethanol for 1 hr followed by UV irradiation and rinsed with PBS and then dried. The cells were seeded on the outside of the tubular scaffold at a cell density of 1×10^5 cells/mL and incubated for 30 minutes in a petri dish. Additional media was added to submerge the scaffold, and the media was changed every 2 days.

2.5 | Cellular infiltration of the scaffold

The scaffolds were cultured with cells for 1, 3, and 7 days. At each time point, the cell cultured scaffolds were cut into ring sections and placed in 10% formalin overnight. The fixed scaffolds were placed into a 30% sucrose solution for 24 hr. The scaffolds were embedded in optimal cutting temperature compound (OCT, Finetek, Torrance, CA). The frozen sections were cut (10 μm) using a cryo-microtome. The sections were stained with DAPI mounting media (Vector Labs, Burlingame, CA). The fluorescent images were taken with an Olympus BX51 microscope, and cell infiltration was measured using Image J software. The cell infiltration was obtained by measuring the distance from the scaffold to the DAPI stain over six random points on the cross-section on three independent sections for each scaffold, and the average of those measurements was the cell infiltration distance.

2.6 | Cell metabolic activity: MTT

The metabolic activity of the cells cultured on the scaffolds was determined by the MTT Vybrant Assay Kit (ThermoFisher Scientific, Waltham, MA) after 1, 3, and 7 days of the cells in culture on the scaffold. A 3 mm diameter punch was used to obtain each sample of the polymer scaffold. Three 3 mm punch-outs were collected for each sample, and then washed with PBS followed by treatment with trypsin that was neutralized with media and serum to detach cells from the scaffold. The cell solution underwent two rounds of centrifugation and PBS washes to remove residual media. The cells were resuspended in PBS to perform the assay per manufacturer protocol. Each sample was used for MTT analysis in a 96-well plate. The samples were incubated at 37˚C for 4 hr with MTT solution at 0.5 mg/mL. After incubation, the unreacted MTT was removed and a solution of dimethylsulfoxide (DMSO) was added to dissolve the formazan crystals for 10 min. Samples were mixed and then the absorbance was measured at 540 nm with a Bio-Rad Microplate Reader.

2.7 | Statistical analysis

All quantitative data are expressed as mean ± *SD*. The statistical difference between individual biodegradable polymer electrospun scaffolds and composite electrospun scaffolds were performed with Student's *t*-test. Cell infiltration data was analyzed using a Mann–Whitney test. MTT data was analyzed using the Student's *t*-test. *p* values less than .05 were considered statistically significant. All statistical analysis was performed using GraphPad Prism 7 software (La Jolla, CA).

3 | RESULTS

3.1 | Scaffold characterization

The composite scaffolds consisting of biodegradable synthetic polymer (PGA, PLGA, and PCL) were electrospun simultaneously as the PEO microparticles were electrosprayed at the same rate (4 mL/hr) on the collecting mandrel. The *SEM* images in Figure 1 compare the scaffold of the electrospun fibers alone (Figure 1a–c) to the fibers after removal of the PEO microparticles (Figure 1d–f). The PEO microparticles are shown in the inserts in Figure 1d–f, and the average diameter of the PEO microparticle was 20–30 μm. The average fiber diameter of the electrospun scaffold was dependent on the type of polymer. The fiber diameters before and after removal of the PEO microparticles are listed in Table 1 (physical properties of electrospun scaffolds). The biodegradable polymers had a similar fiber diameter for the electrospun alone scaffold or the composite scaffold after removal of the PEO microparticle. The random fiber orientation of the electrospun fibers for all the polymers was not affected by the removal of the PEO. The PEO microparticles were integrated throughout the electrospun fiber in a relatively uniform distribution. After exposure of the PEO to the aqueous solution, the PEO particles were completely removed (Figure 1d–f) and the fibers appeared less dense with larger pore sizes compared to the electrospun synthetic polymer alone. The bulk porosity of the electrospun biodegradable polymer scaffold and the composite scaffold after removal of the PEO was calculated by comparing the apparent density of each electrospun scaffold. The bulk porosity of all the biodegradable polymers was significantly increased after the removal of the PEO particles (Table 1). The bulk porosity of the PGA scaffold increased from a baseline of 72% with PGA alone to 90% after the removal of PEO. The PLGA and PCL both started at 61% bulk porosities and after removal of the PEO the PLGA increased to 83% bulk porosity, and the PCL increased to 84% bulk porosity. The increase in porosity was demonstrated by *SEM* and bulk porosity for all three biodegradable polymers.

The complete removal of the PEO microparticles from the electrospun biodegradable scaffolds was verified with Fourier Transform Infrared Spectroscopy (FT-IR) as a chemical test and thermogravimetric analysis (TGA) for physical analysis. A representative FT-IR absorbance spectrum is shown in Figure 2a comparing electrospun PGA alone, the composite scaffold with PEO particle (PGA_{+PEO}), and the composite PGA scaffold after removal of the PEO (PGA_{-PEO}). The PEO spectrum shows a characteristic peak at 2900 cm^{-1} (γ-CH_2) that does not overlap with the PGA spectrum. The composite scaffold demonstrates the peak at 2900 cm^{-1}, and after removal of the PEO, the peak is no longer present. Therefore, the composite after the removal of the PEO from the PGA scaffold is

identical to the spectrum of the electrospun PGA scaffold without any PEO microparticle. Thermogravimetric analysis (TGA) provides data on the physical properties of the polymer that measures the mass of a sample over time as the temperature is increased, and a characteristic TGA curve and melting point are obtained. The melting point of the composite scaffold with the PEO microparticles decreased for all groups compared to the electrospun synthetic polymer alone. A representative TGA thermal curve for PGA is shown in Figure 2b that demonstrated similar thermal curves of the PGA electrospun scaffold alone to the composite PGA electrospun scaffold after the removal of the PEO microparticle. The PLGA and the PCL electrospun scaffolds were observed to have the same effect with similar TGA curves of the electrospun alone scaffold compared to the TGA curve after removal of the PEO microparticle. Therefore, the incorporation of the PEO microparticle and subsequent complete removal of PEO microparticle was demonstrated in a robust manner by visual imaging with *SEM*, chemical structure with FT-IR, and physical property by TGA.

3.2 | Mechanical properties

To determine the effect of removal of the PEO microparticles on the composite electrospun scaffolds, tensile testing of the biodegradable polymer electrospun scaffolds were compared to the composite scaffolds after the removal of PEO microparticles. In Table 1, the biodegradable polymer electrospun and composite scaffold mechanical properties are reported as ultimate tensile strength, Young's Modulus, and extension at break. The crystalline (PGA) and amorphous (PLGA) did not have significant changes in the ultimate tensile strength in the composite scaffold with PEO microparticles. The PLGA scaffold did have a significant reduction in the Young's Modulus and extension to break (Table 1). The more elastic PCL had significant decrease in the ultimate tensile strength and reduction in Young's Modulus. A representative stress–strain curve for PGA alone, PGA with the PEO microparticle, and PGA after removal of the PEO microparticle is shown in Figure 2c.

3.3 | Biodegradation of the scaffolds

The degradation of the biodegradable polymer electrospun scaffold and the composite scaffold after removal of PEO were evaluated by weight change and fiber degradation with *SEM* at 1, 2, and 4 weeks in PBS at 37˚C. As expected, the slower degrading fibers of PLGA and PCL did not have any significant change in fiber diameter (Figure 3d–e,g,h) or weight loss (Figure 3f,i) over the 4 week period. In fact, the PLGA electrospun scaffolds had a slight increase in percent weight that was likely due to fiber swelling in an aqueous solution (Figure 3i). The PGA is a more rapidly degrading polymer, and there was weight loss in both the electrospun scaffold alone and the composite scaffold over the course of the 4 weeks (Figure 3c). The final percent weight loss over the 4 week period for the PGA electrospun scaffold alone was 65% compared to 57% weight loss for the composite PGA scaffold. As shown by the *SEM* images (Figure 3a,b) of PGA fibers at 4 weeks, the fiber length was significantly reduced by hydrolytic degradation with major disruption in the fiber structure. Even at the 2 week time point for PGA (*SEM* data not shown), there was visible breakdown of the fibers with shortening observed. In contrast, the PLGA and PCL did not demonstrate any significant fiber changes in terms of fiber length or diameter.

3.4 | Cell infiltration into the scaffold

The effect of increasing the porosity by the removal of PEO microparticles on the biodegradable electrospun scaffolds was evaluated by comparing the cell infiltration in vitro with human dermal fibroblasts at 1, 3, and 7 days of the biodegradable electrospun scaffold and the composite scaffold. Cellular infiltration was evaluated by cross sections of the polymer scaffolds using a DAPI fluorescent stain (Figure 4). After 1 day, the cell penetration was similar for all the polymer scaffolds in both the biodegradable electrospun scaffold and the composite scaffold. This indicates that at the time of seeding, the increased porosity does not correspond to an increase in the initial penetration into the scaffold. However, by 3 days there is a significant visual difference in the cell migration of the fibroblasts through the composite scaffold compared to the cells remaining mostly on the surface of the biodegradable electrospun scaffolds. The effect of the increased porosity becomes more pronounced by day 7, with the cell infiltration at less than 100 μm through all three biodegradable electrospun scaffolds compared to 300–650 μm for the composite scaffolds after the removal of PEO (Figure 4). The cell migration distance of the cells for all scaffolds over the 7 day culture period was quantified from the cross-section DAPI images and shown in Figure 5. The PGA and PLGA composite scaffolds have a similar depth of cell infiltration by day 7, and the PCL composite scaffold had the most cell infiltration at 650 μm (Figure 5).

3.5 | Cell proliferation within the scaffold

The number of viable cells on the scaffolds at day 3 and 7 were assessed by MTT assay (Figure 6). The MTT assay measures the metabolic activity of cells, and has been used in the setting of electrospun scaffolds as a method to quantify cell number since the metabolic activity is proportional to the cell number. The MTT assay demonstrated a similar trend as the cell infiltration data with a greater number of cells for all the composite scaffolds compared to the biodegradable electrospun scaffold at 3 and 7 days (Figure 6). The total number of cells continued to increase at the day 7 time point compared to the day 3 time point for each set of electrospun scaffolds (Figure 6).

4 | DISCUSSION

Electrospinning is an attractive fabrication method to create nanofiber structures for tissue engineering applications. A challenge for the electrospinning process is to overcome the limitation of the dense packing of the fibers that inhibits cellular infiltration and tissue regeneration. Sacrificial microparticles or nanofibers have been shown with specific biodegradable polymers to increase the porosity of electrospun scaffolds for blood vessels (Wang et al., 2016) and bone tissue regeneration (Francis et al., 2010). We hypothesized that the increase in porosity after removal of the PEO microparticle would increase cellular infiltration for the most common synthetic biodegradable polymers and retain structural stability.

In this study, we developed coelectrospraying PEO microparticle with simultaneous electrospinning for multiple synthetic biodegradable polymers that include PGA, PLGA, and PCL. We characterized the complete removal of the PEO microparticle from the electrospun synthetic biodegradable polymer scaffolds and evaluated the scaffolds by morphology,

mechanical properties, biodegradation, and cell infiltration. The electrosprayed PEO microparticle method has been shown to form a uniform distribution as the microparticles integrate into the electrospun scaffold (Wang et al., 2013), and this feature was demonstrated in this study. Although most studies assess removal of the sacrificial PEO fiber or microparticle by *SEM* (Baker et al., 2008; Wang et al., 2013), we validated the visual removal of the *SEM* by chemical analysis with FT-IR and physical property using TGA. The mechanical properties of the electrospun PLGA and PCL scaffolds did change with the removal of the PEO microparticle, while crystalline electrospun PGA scaffold did not have any significant changes. The PLGA and PCL polymers both had significant reduction in the Young's Modulus, but only the PCL had a decrease in the ultimate tensile strength. There has been a report of a near linear relationship of tensile strength and stiffness to decrease as a sacrificial PEO nanofiber (not microparticle) was removed (Baker et al., 2008). Our data suggests an individual mechanical response for different biodegradable polymers depends on the intrinsic properties of the polymer as the bulk porosity is increased. However, dimensional stability can only be determined either in vitro or in vivo and will also be dependent on the biodegradation of the synthetic polymer. The increase in bulk porosity after the removal of the PEO did not affect the slower degrading PLGA or PCL electrospun scaffolds up to 4 weeks. PGA is known to degrade rapidly (Dong et al., 2010), and the increase in bulk porosity in the electrospun scaffolds after removal of the PEO microparticle resulted in an increase to the surface-to-volume ratio that significantly accelerated the degradation of the PGA scaffolds over 4 weeks.

The effect of increasing the porosity of the PGA, PLGA, and PCL electrospun scaffolds with the removal of PEO was evaluated by assessing the infiltration and proliferation of human dermal fibroblasts seeded on the scaffolds. Human dermal fibroblasts were selected for this study because of the migratory capacity of fibroblasts. Similar to other studies that have reported an increase in cell infiltration with sacrificial PEO microparticles in electrospun scaffolds (Wang et al., 2013; Wang et al., 2014), we found the removal of the PEO microparticles significantly increased cellular infiltration for PGA, PLGA, and PCL electrospun scaffolds over a 7 day culture period. The initial cell migration of the fibroblast cells into the scaffolds with sacrificial PEO had a trend of increased depth at day 1, and by day 3 and 7 there was a significant increase in cell infiltration for all three synthetic polymers with the sacrificial PEO. The MTT data correlated to the cell infiltration data, with significant increase in the number of cells for nearly all the electrospun scaffolds with sacrificial PEO microparticles (except PLGA at day 3) at day 3 and 7. A pore size of at least 10 μm, or the size of a cell, has been suggested to support cell infiltration (Balguid et al., 2009). There is data to suggest fiber diameter may play a stronger role in determining cell infiltration than adding a sacrificial fiber (Zander et al., 2013). However, it is more likely that the sacrificial component will increase cell infiltration when the fiber or particle exceeds the size of the biodegradable polymer fiber to reduce packing density. The fiber diameter was not varied in this study, but there was a range of fiber diameters with the different biodegradable polymers. The lack of response of cell infiltration as fiber diameter increased can be observed in the electrospun biodegradable scaffold alone groups because the depth of cell infiltration was similar for all three biodegradable polymers over 7 days. The polymer with the most cellular infiltration by day 7 was PCL, which was nearly double the

infiltration depth of the PGA and the PLGA. A possible explanation for the greater cell infiltration in the PCL scaffold with sacrificial PEO is the change in pH microenvironment due to degradation byproducts for the PGA and PLGA. Therefore, the primary determinant of fibroblast cell infiltration in the electrospun scaffolds with PGA, PLGA, and PCL was the removal of the sacrificial PEO microparticle.

This study demonstrates the improvement in cell infiltration with the removal of a sacrificial microparticle for three synthetic biodegradable electrospun scaffolds. The use of a sacrificial microparticle does have limitations to enhance porosity in an electrospun scaffold. The size and amount of the microparticle may have to be optimized depending on the cell type, the selected polymer, and the requirements for the biomedical application. A dose response study with the removal of the PEO microparticles could further determine if there is threshold amount of PEO required to augment cell infiltration. A practical consideration with the use of a sacrificial porogen is to remove enough of the porogen above the threshold value for cell infiltration while maintaining dimensional stability of the scaffold. Previous reported studies did correlate the increased cell infiltration with removal of PEO micorparticles in vitro to an in vivo animal model (Wang et al., 2013; Wang et al., 2016), and using an in vivo animal model would further evaluate the potential of improved tissue remodeling with the removal of sacrificial PEO microparticles.

5 | CONCLUSION

The technique of electrospraying with sacrificial PEO microparticles into conventional electrospun scaffolds has been shown to effectively increase porosity of the most common biodegradable polymers thereby enhancing cell infiltration. Even over a wide range of fiber diameters with the PGA, PLGA, and PCL, all of the composite electrospun scaffolds demonstrated an improvement of cell infiltration and proliferation after the removal of the PEO microparticles. The electrospraying technique with a sacrificial PEO microparticle provides another variable along with fiber diameter to customize the porosity and mechanical properties of the electrospun scaffold. A limitation of this study is the variation in the fiber diameter of the electrospun scaffolds with each biodegradable polymer. The effect of fiber diameter could be further characterized with another study by varying the fiber diameter of the electrospun scaffold with and without the PEO microparticle. Additional studies would need to be performed to investigate the PEO microparticle ratio to the electrospun biodegradable polymer to optimize the cell infiltration, biodegradation, and mechanical properties for specific clinical applications. This study demonstrates that PEO microparticles can be used across a wide variety of synthetic biodegradable electrospun scaffolds to improve cell infiltration with stable mechanical properties for tissue regeneration.

ACKNOWLEDGMENTS

This study was supported in part by an NIH Clinical and Translational Science Award grant (UL1 TR000001, formerly UL1RR033179), awarded to the University of Kansas Medical Center.

REFERENCES

Agarwal S, Wendorff JH, & Greiner A (2009). Progress in the field of electrospinning for tissue engineering applications. Advanced Materials, 21, 3343–3351. [PubMed: 20882501]

Baker BM, Gee AO, Metter RB, Nathan AS, Marklein RA, Burdick JA, & Mauck RL (2008). The potential to improve cell infiltration in composite fiber-aligned electrospun scaffolds by the selective removal of sacrificial fibers. Biomaterials, 29, 2348–2358. [PubMed: 18313138]

Balguid A, Mol A, van Marion MH, Bank RA, Bouten CV, & Baaijens FP (2009). Tailoring fiber diameter in electrospun poly(epsilon-caprolactone) scaffolds for optimal cellular infiltration in cardiovascular tissue engineering. Tissue Engineering. Part A, 15, 437–444. [PubMed: 18694294]

Barnes CP, Sell SA, Boland ED, Simpson DG, & Bowlin GL (2007). Nanofiber technology: Designing the next generation of tissue engineering scaffolds. Advanced Drug Delivery Reviews, 59, 1413–1433. [PubMed: 17916396]

Carletti E, Motta A, & Migliaresi C (2011). Scaffolds for tissue engineering and 3d cell culture. Methods in Molecular Biology, 695, 17–39. [PubMed: 21042963]

Dong Y, Yong T, Liao S, Chan CK, Stevens MM, & Ramakrishna S (2010). Distinctive degradation behaviors of electrospun polyglycolide, poly(dl-lactide-co-glycolide), and poly(l-lactide-co-epsilon-caprolactone) nanofibers cultured with/without porcine smooth muscle cells. Tissue Engineering. Part A, 16, 283–298. [PubMed: 19839726]

Francis L, Venugopal J, Prabhakaran MP, Thavasi V, Marsano E, & Ramakrishna S (2010). Simultaneous electrospin-electrosprayed biocomposite nanofibrous scaffolds for bone tissue regeneration. Acta Biomaterialia, 6, 4100–4109. [PubMed: 20466085]

Ju YM, Choi JS, Atala A, Yoo JJ, & Lee SJ (2010). Bilayered scaffold for engineering cellularized blood vessels. Biomaterials, 31, 4313–4321. [PubMed: 20188414]

Langer R, & Vacanti JP (1993). Tissue engineering. Science, 260,920–926. [PubMed: 8493529]

Leong MF, Rasheed MZ, Lim TC, & Chian KS (2009). In vitro cell infiltration and in vivo cell infiltration and vascularization in a fibrous, highly porous poly(d,l-lactide) scaffold fabricated by cryogenic electrospinning technique. Journal of Biomedical Materials Research. Part A, 91, 231–240. [PubMed: 18814222]

Li M, Mondrinos MJ, Gandhi MR, Ko FK, Weiss AS, & Lelkes PI (2005). Electrospun protein fibers as matrices for tissue engineering. Biomaterials, 26, 5999–6008. [PubMed: 15894371]

Li WJ, Cooper JA Jr., Mauck RL, & Tuan RS (2006). Fabrication and characterization of six electrospun poly (alpha-hydroxy ester) based fibrous scaffolds for tissue engineering applications. Acta Biomaterialia, 2, 377–385. [PubMed: 16765878]

Matthews JA, Wnek GE, Simpson DG, & Bowlin GL (2002). Electrospinning of collagen nanofibers. Biomacromolecules, 3, 232–238. [PubMed: 11888306]

Nam J, Huang Y, Agarwal S, & Lannutti J (2007). Improved cellular infiltration in electrospun fiber via engineered porosity. Tissue Engineering, 13, 2249–2257. [PubMed: 17536926]

Pham QP, Sharma U, & Mikos AG (2006). Electrospinning of polymeric nanofibers for tissue engineering applications: A review. Tissue Engineering, 12, 1197–1211. [PubMed: 16771634]

Phipps MC, Clem WC, Grunda JM, Clines GA, & Bellis SL (2012). Increasing the pore sizes of bone-mimetic electrospun scaffolds comprised of polycaprolactone, collagen i and hydroxyapatite to enhance cell infiltration. Biomaterials, 33, 524–534. [PubMed: 22014462]

Sell SA, McClure MJ, Barnes CP, Knapp DC, Walpoth BH, Simpson DG, & Bowlin GL (2006). Electrospun polydioxanoneelastin blends: Potential for bioresorbable vascular grafts. Biomedical Materials, 1, 72–80. [PubMed: 18460759]

Wang K, Xu M, Zhu M, Su H, Wang H, Kong D, & Wang L (2013). Creation of macropores in electrospun silk fibroin scaffolds using sacrificial peo-microparticles to enhance cellular infiltration. Journal of Biomedical Materials Research. Part A, 101, 3474–3481. [PubMed: 23606405]

Wang K, Zheng W, Pan Y, Ma S, Guan Y, Liu R, … Kong D (2016). Three-layered pcl grafts promoted vascular regeneration in a rabbit carotid artery model. Macromolecular Bioscience, 16, 608–618. [PubMed: 26756321]

Wang K, Zhu M, Li T, Zheng W, Li L, Xu M, … Wang L (2014). Improvement of cell infiltration in electrospun polycaprolactone scaffolds for the construction of vascular grafts. Journal of Biomedical Nanotechnology, 10, 1588–1598. [PubMed: 25016658]

Wu J, & Hong Y (2016). Enhancing cell infiltration of electrospun fibrous scaffolds in tissue regeneration. Bioactive Material, 1, 56–64.

Zander NE, Orlicki JA, Rawlett AM, & Beebe TP Jr. (2013). Electrospun polycaprolactone scaffolds with tailored porosity using two approaches for enhanced cellular infiltration. Journal of Materials Science. Materials in Medicine, 24, 179–187. [PubMed: 23053801]

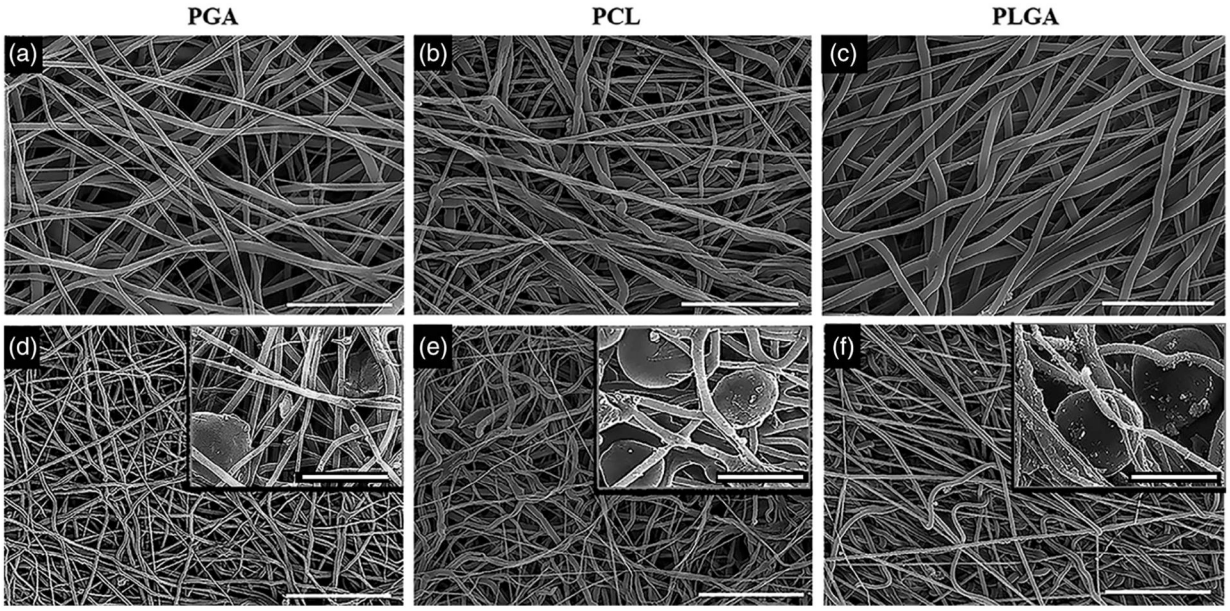

FIGURE 1.

Scanning electron microscope micrographs of the individual biodegradable electrospun scaffolds and composite electrospun scaffolds. (a) PGA electrospun scaffold. (b) PCL electrospun scaffold. (c) PLGA electrospun scaffold. The composite electrospun scaffolds with microparticles in the insert. (d) Composite PGA. (e) Composite PCL. (f) Composite PLGA. Scale bar: (a) 7.5 μm (b,c) 20 μm (d–f) 50 μm; insert (a–f) 25 μm

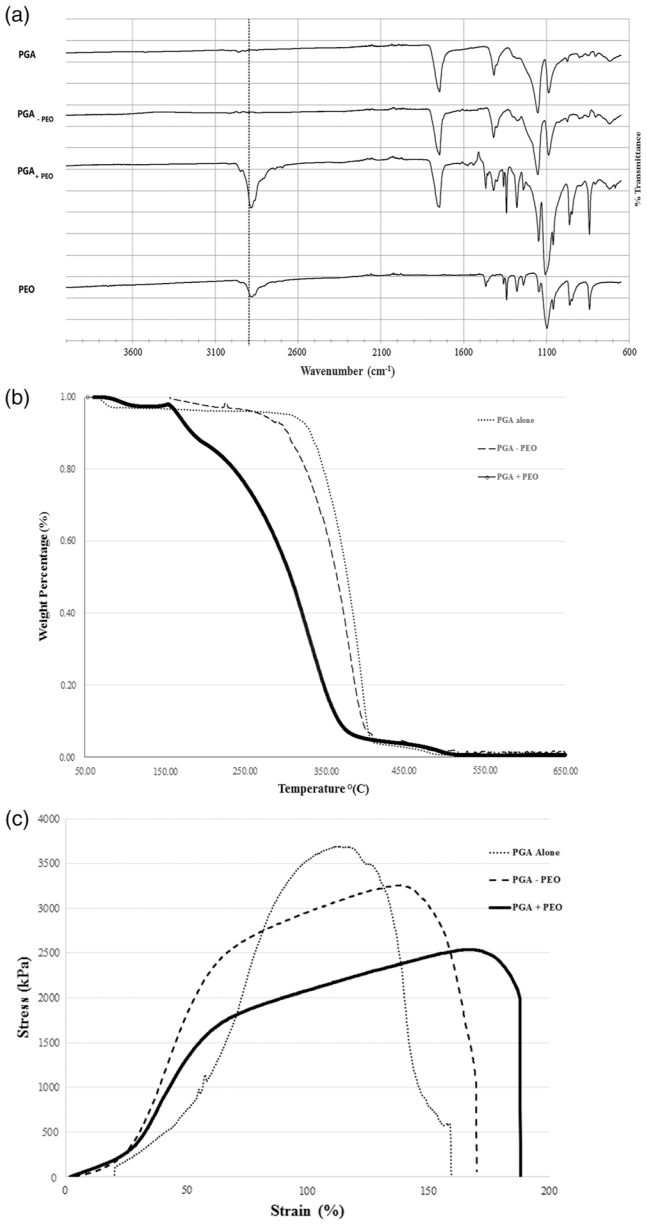

FIGURE 2.

(a) Fourier transform infrared spectroscopy of electrospun PGA scaffold, the composite scaffold without PEO (PGA $_{-PEO}$), the composite PGA scaffold with PEO prior to removal (PGA $_{+PEO}$), and electrosprayed PEO scaffold only. The peaks noted with the dotted lines are characteristic of PEO. (b) TGA thermal curve comparing electrospun scaffold with PGA alone, PGA plus PEO microparticle, and PGA minus PEO microparticle. (c) Stress–strain curve for electrospun PGA alone, PGA plus PEO microparticle, and PGA minus PEO microparticle

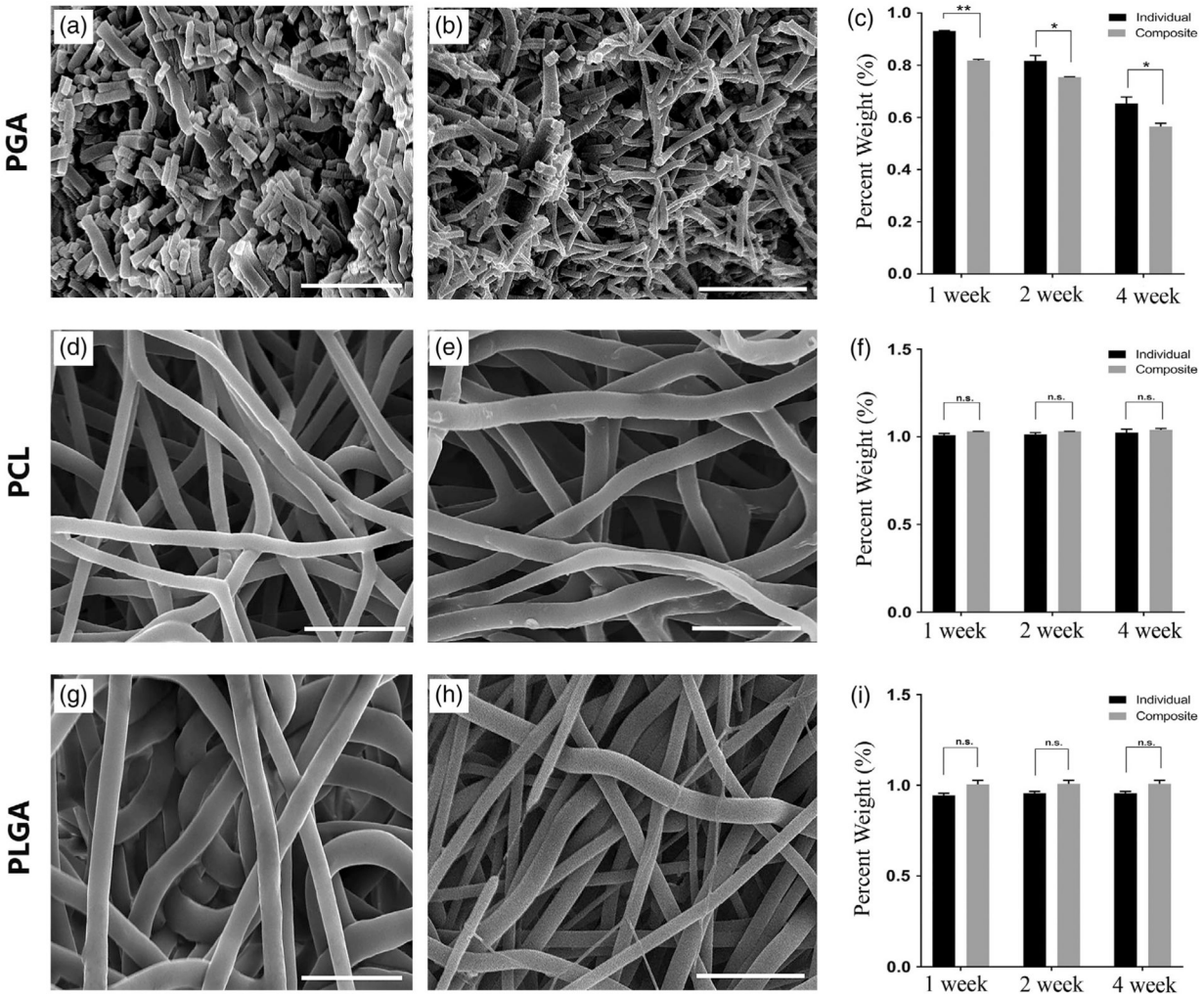

FIGURE 3.

Biodegradation of the electrospun and composite PGA, PCL, and PLGA scaffolds. The first column is *SEM* images of the electrospun scaffold alone for each polymer at 4 weeks: (a) PGA, (d) PCL, (g) PLGA; the second column is the *SEM* images of the composite electrospun scaffold after removal of the PEO microparticle at 4 weeks: (b) PGA, (e) PCL, (h) PLGA. The third column is a chart of retained weight of the electrospun or composite scaffold for (c) PGA, (f) PCL, (i) PLGA at time points of 1, 2, and 4 weeks. Scale bar: 15 μm. n.s. is not statistically significant; *Significant difference, $p < .05$; **Significant difference, $p < .01$

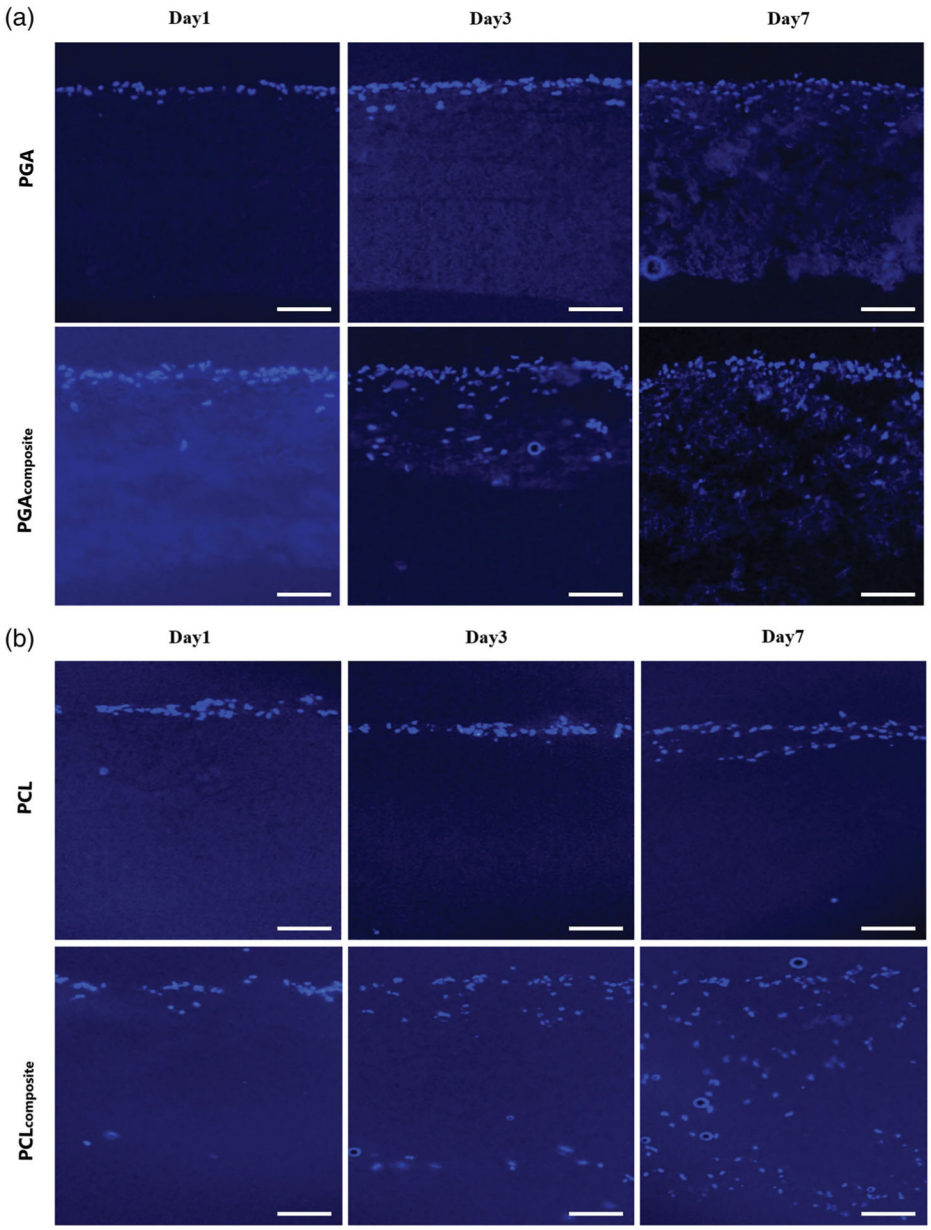

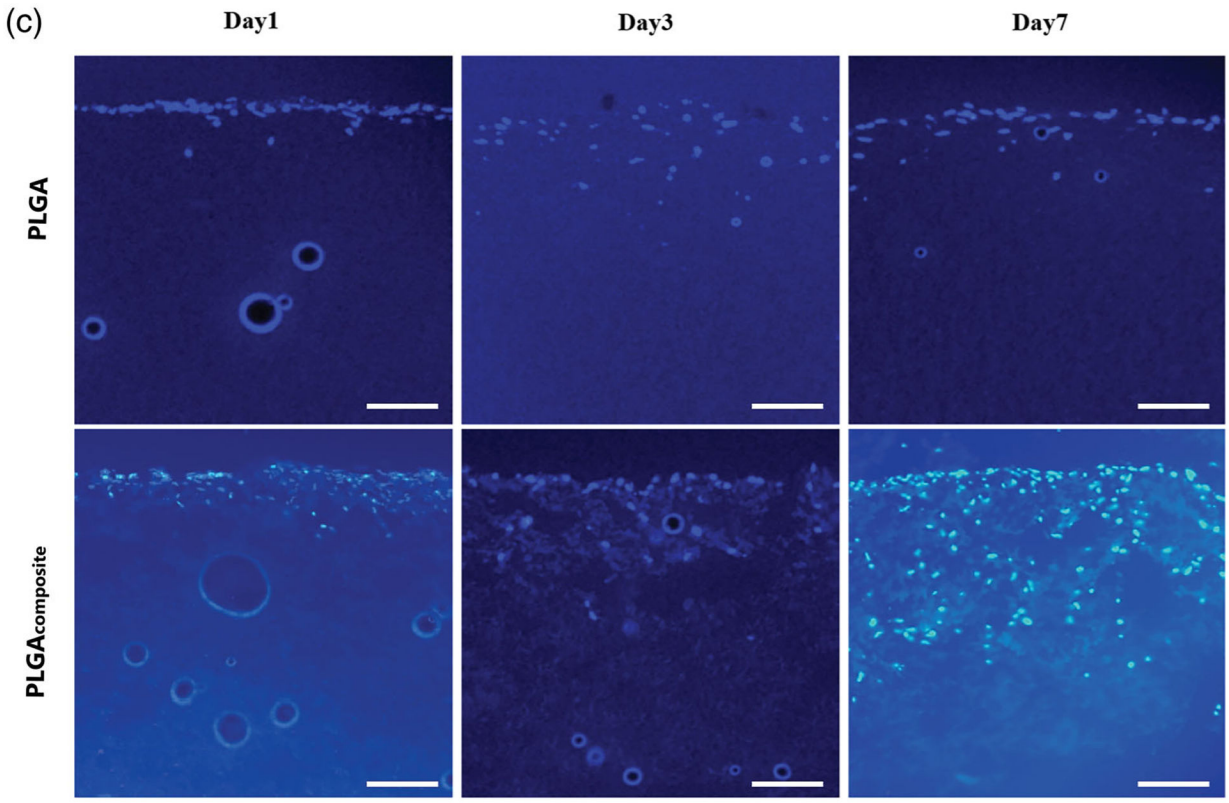

FIGURE 4.

The cross-section histology of the fibroblast cell infiltration into the electrospun and composite scaffolds with DAPI staining (cell nuclei) on a fluorescent microscope at day1, 3, and 7. (a) PGA, (B) PCL, (C) PLGA. Scale bar: 100 μm (all images)

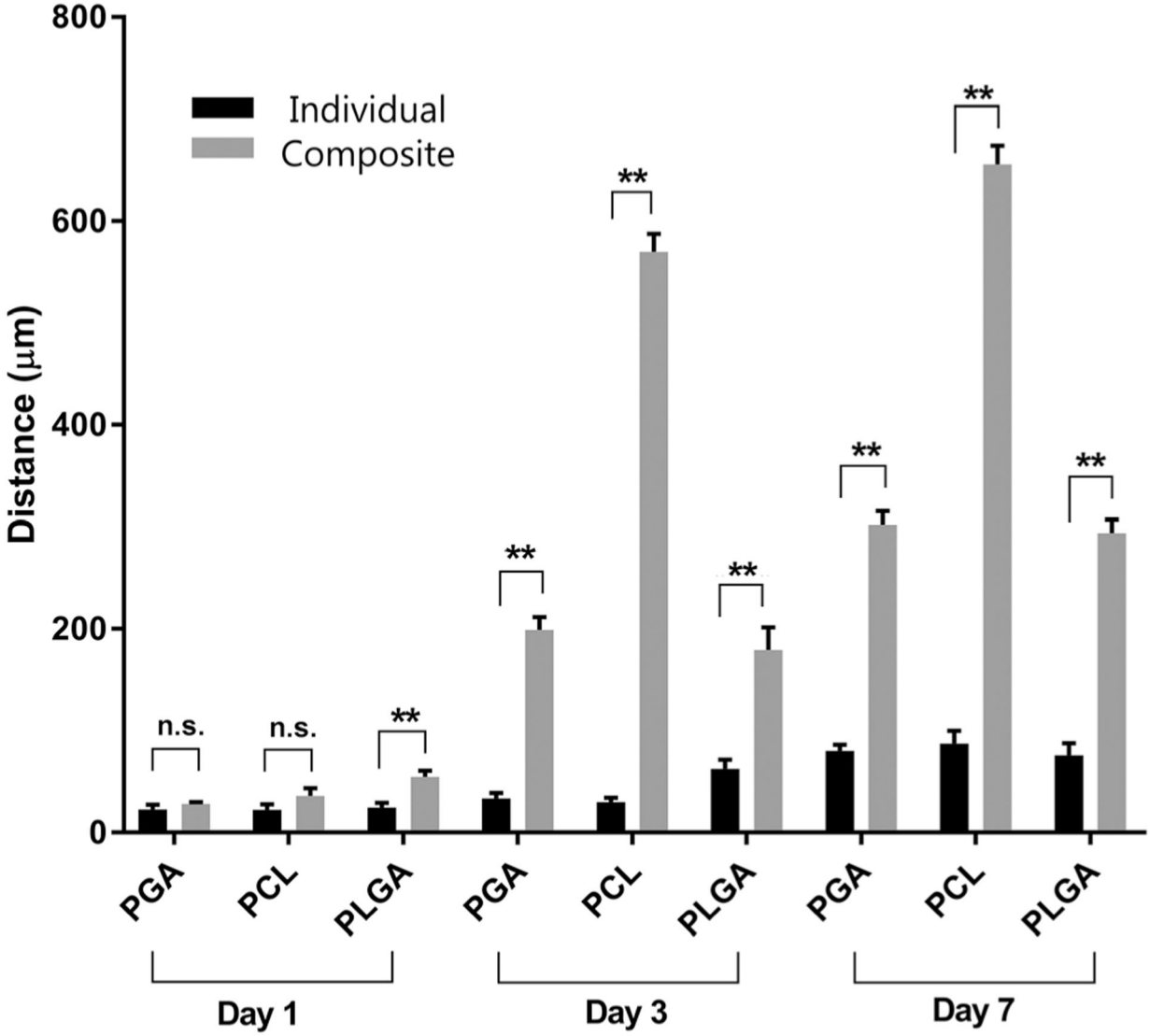

FIGURE 5.

Fibroblast cell infiltration into the electrospun and composite PGA, PCL, PLGA scaffolds with quantitative analysis from the cross-section at 1, 3, and 7 days. N.s. is not statistically significant; **Significant difference, $p < .01$

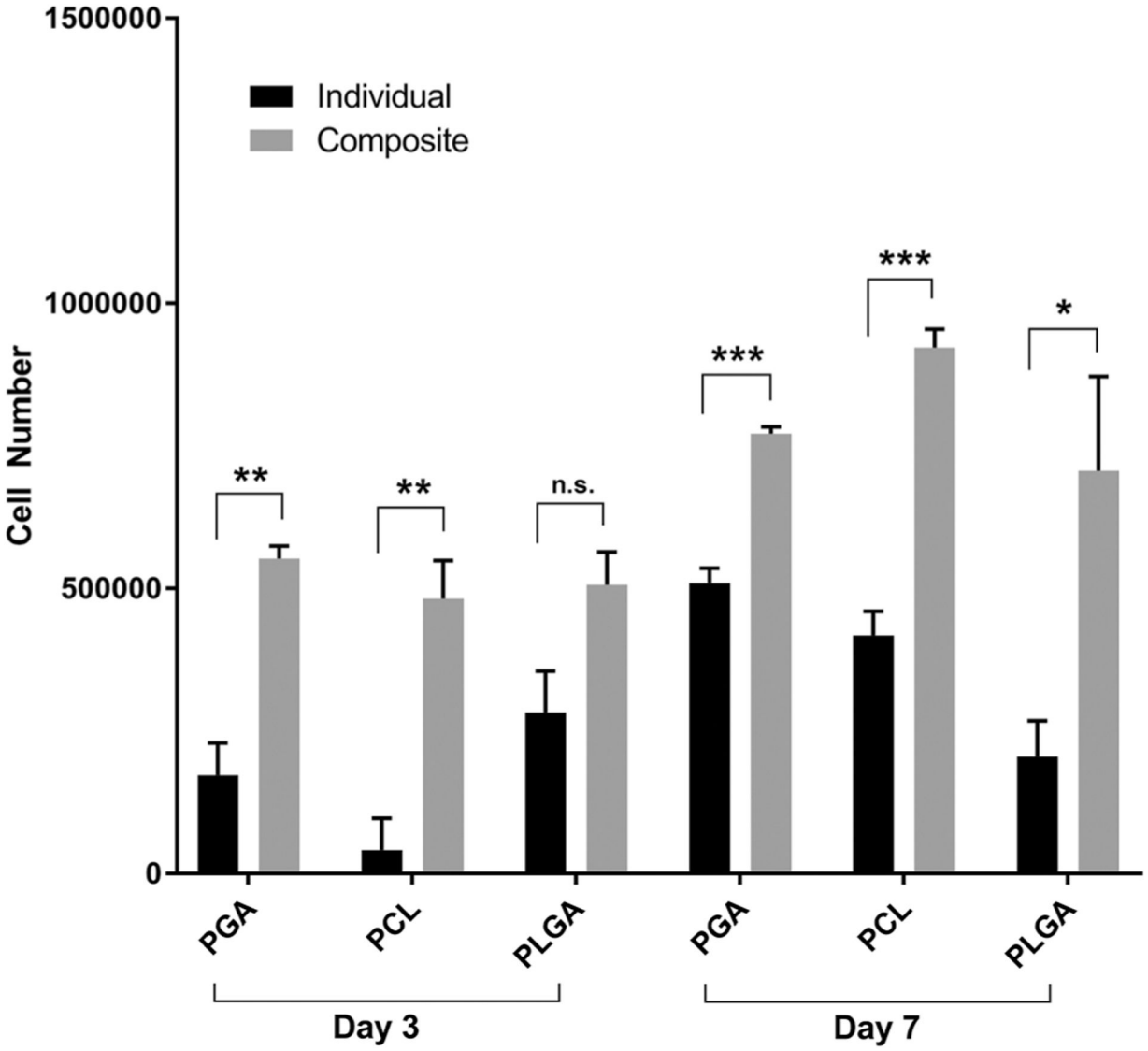

FIGURE 6.

Metabolic activity of the fibroblast cells on the electrospun and composite PGA, PCL, PLGA scaffolds at day 3 and day 7 with MTT assay. N.s. is not statistically significant; *Significant difference, $p < .05$; **Significant difference, $p < .01$; ***Significant difference, $p < .001$

TABLE 1

Physical properties of electrospun scaffolds

	Image analysis (n = 4)	Mechanical testing (n = 3)			Physical analysis	
Scaffold	**Fiber diameter (nm)**	**Ultimate tensile strength (kPa)**	**Young's modulus (kPa)**	**Extension at break (%)**	**Melting range (°C)**	**Porosity**
PGA	666 ± 168	3,448 ± 653	74 ± 3	152 ± 23	310–410	72%
$PGA_{Composite}$	609 ± 177	3,322 ± 246	66 ± 3	171 ± 5	300–410	90%
PCL	1,165 ± 352	7,051 ± 942	28 ± 3	453 ± 46	360–440	61%
$PCL_{Composite}$	1,171 ± 329	2,571 ± 439	9 ± 1	488 ± 49	370–440	83%
PLGA	2,211 ± 585	5,908 ± 247	141 ± 15	276 ± 22	290–380	61%
$PLGA_{Composite}$	2,294 ± 633	6,043 ± 623	86 ± 15	144 ± 9	290–390	84%

J Biomed Mater Res A. Author manuscript; available in PMC 2020 March 23.